

Coupled response of compliant offshore platforms

J. W. Leonard and R. A. Young

*Ocean Engineering Program, Oregon State University, Corvallis, OR 97331, USA
(Received May 1984; revised October 1984)*

A three-dimensional finite element analysis has been used to simulate the coupled static and dynamic behaviour of compliant ocean structures. Nonlinearities which result from large deflections, reduced or zero stiffness in compression, and nonconservative fluid loading are considered. The spatial variation of fluid loading is also addressed. The structures are assumed to be in the Morison regime. Linear wave theory is used and multidirectional seas may be simulated. A variable current profile may be specified and concentrated masses and loads, as well as foundation properties, may be modelled. Updated Lagrangian coordinates and a residual feedback, incremental-iterative, solution is adopted. Viscous relaxation is used to start the static solution of problems with small initial stiffnesses. The dynamic solution is performed in the time domain and uses the Newmark integration scheme. Consistent mass matrices are developed for both beam-column and cable elements. The directionality of the hydrodynamic added mass is accounted for, as is the discontinuity of the mass density for elements which pierce the water surface. Examples are presented of an articulated tower, of a guyed tower, and of a tension leg platform.

Key words: offshore construction works, static response, dynamic response

The economic production of petroleum in deep water requires structures which often test the limits of existing technology. Compliant production platforms are one such class of deep water structures. Since they are compliant, these structures must be designed dynamically. Also, since they are exposed to loads which vary in a nonlinear way and are themselves mechanisms which behave in a nonlinear manner, their analysis is highly complex. In this study a finite element model is developed which deals with nonlinear dynamic problems of compliant platforms.

A compliant ocean structure is one which moves significant lateral distances when subject to wave and wind loadings. It relies upon its dynamic softness to reduce maximum transmitted anchorage loads. Unlike the fixed structure where structural velocities and accelerations are small and the time-varying wind and wave loads may be treated as a time series of static problems, the compliant structure has significant kinematics and the role of structural mass, added mass, and damping must be considered.

Compliant tower concepts

Compliant structure concepts may be classified in one of four categories:

- Articulated towers
- Guyed towers
- Tension-leg platforms
- Floating production facilities

The concepts differ mainly in the means by which the loadings are transmitted to the seabed and in the form of the anchorage to the sea floor. They all resemble inverted pendulums, with excess buoyancy replacing gravity loads.

The articulated tower consists of a vertical column to which buoyancy has been attached near the water surface and to which ballast is usually added near the bottom. The tower is connected to the sea floor through an articulated hinge joint to a base which may be of either piled or gravity-type. The tower itself may be either a tubular

column or a trussed steel latticework. The structure is dynamically tuned to have a natural period removed from periods of high wave energy.

The articulated tower was among the first of the more elaborate compliant designs to see ocean service. It is presently being used as single point mooring and loading terminals, control tower and flare structures and, coupled to a resident tanker, as early production facilities in the North Sea and in the Atlantic Ocean. The structure is typically designed for water depths of 200–600 ft (65–200 m) but concepts have been developed for water depths in excess of 1200 ft (400 m). The dynamics of articulated tower^{1–3} structures in two and three dimensions have been explored.

The guyed tower is a rectangular lattice column connected to the sea floor by either a piled foundation or a gravity-type foundation. The tower is long and slender and depends upon a group of relatively slack guy lines for lateral stability in resisting wave and wind loads. An important distinctive feature of the guys is the clump weights which are attached to the cable guys and which initially are at rest on the sea floor some distance from both the tower and the cable anchors. Since it is desired from operating requirements to have a relatively stiff system for normal sea conditions the tower is tensioned to be fairly rigid and the clump weights are sized to remain on the bottom. In survival sea conditions, the system becomes more compliant when the clump weights leave the bottom.

A guyed tower was first constructed as an instrumented model in 293 ft (89 m) of water^{4,5} in the Gulf of Mexico. Test data showed that a simplified analysis would not adequately describe the kinematic and dynamic response of the structure as a function of time. Recent work⁶ has considered the nonlinearities of the combined analysis of tower and guys in a hydrodynamic environment. A nonlinear stochastic analysis of a tower using spring idealizations for guys has been performed using the Fokker-Planck equation.⁷ Currently, simplified models are being developed that are suitable for parametric study.⁸

The tension-leg platform is a semisubmersible vessel which is moored to the sea floor by a number of pretensioned vertical tendons connected to a template which is piled in place. Like the articulated towers, these structures are free to move in surge and sway. They also have a more limited freedom in yaw, while roll, pitch, and heave are severely restricted by the pretensioned tendons. The natural periods of the structure in surge, sway and yaw must be greater than the wave periods of significant energy. The heave, roll and pitch natural periods, on the other hand, being much shorter, must be less than the significant wave energy periods.

A tension-leg platform^{9,10} first saw ocean service in 1974. The nonlinear dynamics of the tension-leg platform have been considered^{11,12} in terms of a Mathieu-Hill equation. While many investigators were examining instabilities of tension-leg platforms,^{13–17} others^{18–20} were examining computational techniques for both linearized frequency-domain analyses and time-domain solutions.

Floating production facilities are similar to tension leg platforms in that they both use a semisubmersible vessel as a platform. They differ by having a catenary-type of anchoring system rather than tendons. The structure is free to move with relatively larger amplitudes in the roll-pitch-heave modes. It is required that natural periods in all modes be removed from significant wave energy periods. Floating production facilities have been in service since

1975 in the North Sea. Ten such units are presently in operation worldwide.

Objectives

In this paper an algorithm for the nonlinear coupled analysis of a compliant guy-structure system in the ocean is presented. There exists a significant amount of work dealing with separate components of the structure. The dynamic response of the platform, governed by the Morison equation with cables modelled as springs, has been treated.^{21–24} Likewise, many investigators^{14,25–28} have analysed catenary moorings using either finite elements or finite differences.

Generally the motions of the guy-structure system are determined in a decoupled procedure wherein the guys are first represented by springs with load-deflection characteristics similar to those of the static guy system. The platform is then dynamically analysed using these representations. The resulting motions of the platform are then applied to a dynamic model of the guy cluster and the resulting loads in the cable-to-tower connection are compared to those of the spring-platform analysis.

There is a problem in that approach: it is presupposed that the procedure is valid and the results are forced to fit an assumed character. Since the coupled dynamic problem involves numerous nonlinearities, it is difficult to assess the validity of the assumptions of decoupled analysis in a qualitative manner.

Model tests of guys and theoretical calculations indicate that there is a need for a coupled analysis which incorporates the nonlinear behaviour of the total system.⁶ One main reason is that theoretical work indicates that there is hysteretic energy dissipated in the guy system. Certainly, hydrodynamic drag loads on the cables are energy dissipators, and they are spatially and directionally dependent. Not only are the drag loads dependent on the spatial orientation of the cable but they are also dependent on the directionality of the waves or current, being greater when moving against the waves or current. A nonlinear coupled analysis which can deal with such phenomena provides a means to quantitatively assess the validity of decoupling assumptions and also the range of that validity.

The algorithm used in the computer program developed during the course of this work is a residual feedback scheme. This is an incremental and iterative technique in which the load may be applied in steps with a full Newton-Raphson iteration to convergence at each step. Static problems with low initial stiffness are considered using a viscous relaxation procedure incorporated into the algorithm. An implicit scheme is used for the numerical integration in time.

Basic concepts and assumptions

The compliant structure is, in general, a complex one, being composed of many different elements, chain, cable, rope, tubulars, structural sections, plate, etc. In addition, the loadings are a complex interaction of gravity, buoyancy, waves, current, wind and seismic activity. It is necessary to make certain simplifying assumptions. Derivation of the element stiffness matrices is carried out using the principle of virtual displacements and the Rayleigh-Ritz method of approximate solution.²⁹ Mass matrices may be derived in a manner analogous to the stiffness matrices by means of D'Alembert's principle.

Beam-column element

The primary components of the compliant platform are the beam-column elements which approximate the rigid support frame. They are subject to the following restrictions:

Elements are composed of a linearly elastic material. Although the beam-column elements may undergo large displacements, deformations are assumed to be sufficiently small for small-deflection theory to be valid within the elements.

Elements are considered to be sufficiently long for transverse deformations due to shear to be negligible compared to those due to bending.

Bending moments of inertia about the major and minor axes need not be the same, and polar moments of inertia may be independent of bending moments of inertia.

Hydrodynamic coefficients are assumed to be independent of the orientation of the beam and are assumed to apply to an axisymmetric body. No account is taken of variation in Reynolds number or Keulegan-Carpenter number within the flow.

The beam-column is a two-noded straight element.

Deformation of the element is described by three translational and three rotational degrees-of-freedom at each node. The displacement or location of the element is described solely by the three translational degrees-of-freedom. The element is thus subparametric and it is derived using small deflection approximations, but accounting for the nonlinear effect of axial load on bending stiffness. The resulting stiffness matrix consists of a linear part, as given by numerous authors,²⁹ and a nonlinear part, known as the geometric stiffness matrix, given in Table 1.

Calculation of the internal load for the beam element is complicated by the fact that the nodes have rotational degrees-of-freedom. Implicit in the assumption of small-deflection theory is the use of small angle approximations. The internal loads are calculated using the instantaneous

Table 1 Geometric stiffness matrix for beam F_1 = force in element, L = length

	0		0		
	$\frac{36}{L^2}$		$\frac{3}{L}$	$-\frac{36}{L^2}$	$\frac{3}{L}$
	$\frac{36}{L^2}$	$\frac{3}{L}$		$-\frac{36}{L^2}$	$\frac{3}{L}$
	0		0		
		$4L$		$-\frac{3}{L}$	$-L$
$\frac{F_1 L}{30}$		$4L$	$-\frac{3}{L}$		$-L$
		0		$\frac{36}{L^2}$	$-\frac{3}{L}$
				$\frac{36}{L^2}$	$-\frac{3}{L}$
	Sym			0	$4L$
					$4L$

stiffness matrix and nodal displacements. When the element undergoes large rigid body rotations, the use of the total rotational angle will lead to erroneous results since the small angle approximations are no longer valid. To correctly calculate the internal load using updated Lagrangian coordinates and the small-deflection element, it is necessary to calculate the relatively large rigid body rotations and then subtract them from the total nodal rotations. The resultant relative angles of rotation are small, provided the structure is initially well proportioned, or provided the discretization is sufficiently fine.

Cable element

The second structural element found on most compliant structures is the guy, or cable, element which provides lateral stability to the structure. Cables behave in an inherently geometrically nonlinear fashion and linear approximations are sufficient only for problems with small deflections and low sag-to-span ratios. The cable elements of this analysis are subject to the following assumptions:

The cable elements are composed of a linearly elastic material and are assumed to possess negligible flexural and torsional stiffnesses.

In the slack condition, determined by the absence of tension, zero structural stiffness is assumed, but inertia loads due to cable mass and added mass are transmitted to the connecting structure.

The cables are assumed to be cylindrical in shape and hydrodynamic load coefficients are assumed to be independent of cable orientation and local kinematics of water particles.

The cable is a straight two-noded isoparametric element in which both displacement and deformation are described by nodal translations. Tuah³⁰ derived the linear and nonlinear stiffness matrices for updated Lagrangian coordinates in the global reference frame. The stiffness matrix is given by:

$$K = \frac{T}{L} \begin{bmatrix} I & -I \\ -I & I \end{bmatrix} + \frac{A_0 E}{L_0 L^2} \begin{bmatrix} C & -C \\ -C & C \end{bmatrix} \quad (1)$$

where T is the cable tension, L is the element length in the updated configuration, A_0 = initial area, E = elastic modulus, I = 3 x 3 identity matrix, and:

$$C_{ij} = x_i^b x_j^b + x_i^e x_j^e - x_i^b x_j^e - x_i^e x_j^b$$

The values x_i^b and x_i^e are the instantaneous global coordinates of the beginning node and end node, respectively, of the element.

Foundation element

The compliant platform is eventually anchored to the sea floor by one or more of a variety of foundation devices. There is, of course, interaction between the sea floor and the structural anchorage. To account for this interaction a simple foundation element is used. It is subject to the following restrictions:

Foundation stiffness is linear over the range of applied loads and may have different stiffnesses in each of the six degrees-of-freedom.

Energy dissipation by the soil is assumed to occur as equivalent viscous damping, with the damping parameters specified separately for each of the six degrees-of-freedom.

Any effective mass of the foundation must be represented as a lumped mass at the foundation to structure connection, and hydrodynamic loads on the foundation are ignored.

Loads

In addition to gravity loads the compliant structure is influenced by buoyancy, waves, currents, tides, wind loads, seismic loads and a variety of live loads peculiar to the purpose of the structure. Only loads due to gravity, buoyancy, waves and currents are considered in this work. The buoyancy force is applied to all members for which displaced volume is specified and is applied only to those elements or portions of elements which lie below the still water level.

Wave loads on a differential segment of a cylinder are calculated using a generalized form of the Morison equation which accounts for orientation of the cylinder axis and for relative motions of the fluid and the structure:³¹⁻³⁴

$$dF_i^w = \left[\frac{1}{2} \rho C_D D |\dot{u}_i^N - \dot{q}_i^N| (\dot{u}_i^N - \dot{q}_i^N) + \frac{\pi}{4} \rho (C_a + 1) D^2 \ddot{u}_i^N - \frac{\pi}{4} \rho C_a D^2 \ddot{q}_i^N \right] dx_i' \quad (2)$$

where \dot{q}_i^N and \ddot{q}_i^N are the components of cylinder velocity and acceleration normal to its axis, ρ is density, D is diameter, \dot{u}_i^N and \ddot{u}_i^N are the components of fluid velocity and acceleration normal to the axis and dx_i' are components of differential distance along the axis. The parameter C_D is the empirical drag coefficient and C_a is the added mass coefficient.

Current loads without waves

In the ocean, current direction need not coincide with wave direction and may vary with depth. The speed may also change with depth. To permit a realistic description, a profile which may vary in both magnitude and direction with depth is considered. The current is assumed to be steady and to have no vertical component.

Combined wave and current loads

Wave and current loadings naturally occur simultaneously. An exact treatment of their combined kinematics is a complicated problem. Fortunately, a simple superposition scheme has been shown to be adequate³⁵ for most situations when the Morison equation is used. Provided that the particle velocities are summed before calculating the drag load, the nonlinear effects due to the interaction of current and wave are negligible.³⁶ When the drag force is properly accounted for the combined force equations becomes:

$$F_i^H = \int_L \left[\frac{1}{2} \rho C_D D |\dot{u}_i^N + \dot{v}_i^N - \dot{q}_i^N| (\dot{u}_i^N + \dot{v}_i^N - \dot{q}_i^N) + \frac{\pi}{4} \rho (C_a + 1) D^2 \ddot{u}_i^N - \frac{\pi}{4} \rho C_a D^2 \ddot{q}_i^N \right] dx_i' \quad (3)$$

where \dot{v}_i^N are components of steady current velocity normal to the axis.

Linear wave theory is used with no adjustment for free surface effects. When a current is present, the wave characteristics need to be modified to reflect the current upon

which the wave is superimposed. If the current is uniform, one may derive the kinematics in a reference frame moving at a constant velocity which freezes the wave form with respect to time.³⁴ If the current profile varies with depth, the problem is more complicated.³⁷ An *ad hoc* procedure is used here to account for the apparent wave frequency shift. A weighted average current in the wave direction is calculated.

Load discretization

Concentrated loads are applied directly to the nodes but distributed loads on elements due to gravity, buoyancy, current, and waves must be transformed to equivalent loads applied at the nodes. The nodal loads that are sought are those which, if applied to the element at the nodes, would produce the same strain energy in the element as the distributed load would when the element nodal degrees-of-freedom are fixed. These fixed-end forces may be derived using virtual displacement principles. For one-dimensional elements such as the cable and the beam, exact solutions are possible and the nodal forces are recognized as the fixed-end forces of elementary structural analysis.

Buoyancy loads are assumed to act over elements with constant cross-section and hence with uniform displaced volume. But, since elements may pierce the surface, the buoyancy load is not necessarily continuous over the entire length of the element. Hydrodynamic loading may also be discontinuous for the same reason, and the loading is generally not uniform over the submerged part of the element. To allow the use of reasonably large elements and to produce an accurate load profile for arbitrarily defined combinations of wave, current, and buoyancy, an influence function is used to calculate the fixed-end forces. If the reactions due to a point load of unit magnitude on the element are known, the reactions from any load distribution may be calculated as the sum of the reactions due to a series of point loads whose magnitudes are determined by the loading function.

To permit the use of an arbitrary current profile and also to reduce computational effort, the hydrodynamic load intensities are calculated at a fixed number of equally spaced elevations from sea bottom to the still water line. Between each elevation, load intensity is assumed to vary linearly. The fixed-end forces are calculated by first interpolating to find the load intensity at the end nodes of the submerged element and to find the location with respect to the beginning node of the remaining calculated load intensities. Then the fixed-end forces due to each trapezoidal load prism are calculated.

Equations of motion

Newton's second law for a multiple degree-of-freedom system may be written in component notation as:

$$M_{ij} \ddot{q}_j + C_{ij} \dot{q}_j + K_{ij} q_j = F_i^H(t) + F_i^s \quad (4)$$

where the force vector is composed of the restoring force $K_{ij} q_j$, the structural damping force, $C_{ij} \dot{q}_j$, the forcing function $F_i^H(t)$ and any steady loads F_i^s . M_{ij} is the mass matrix, K_{ij} is the structural stiffness matrix, C_{ij} is the structural damping matrix and q_j is the vector of structural displacements.

Since structural damping is generally assumed small with respect to hydrodynamic damping, the second term in equation (4) is neglected in this work. Integration of

equation (3) over the length of the member, L , and substituting the result into (4) leads to the relation:

$$M_{ij}\ddot{q}_j + K_{ij}q_j = \left[\frac{1}{2}\rho C_D D |V_i^N| (\dot{u}_i^N + \dot{v}_i^N - \dot{q}_i^N) + \frac{\pi}{4}\rho(C_a + 1) D^2 \ddot{u}_i^N - \frac{\pi}{4}\rho C_a D^2 \ddot{q}_i^N \right] L + F_i^s \quad (5)$$

where:

$$|V_i^N| = \sum_{j=1}^3 (\dot{u}_j^N + \dot{v}_j^N - \dot{q}_j^N)^2)^{1/2} \quad (6)$$

is the resultant relative velocity of node i .

Solution methods

For large-deflection statical problems, the stiffness matrix becomes a function of the displacement vector:

$$F_i = K_{ij}(q_k) q_j \quad (9)$$

Generally the nonlinear problem is solved by first linearizing the nonlinear relationship and then performing some form of incremental, or iterative, or combined incremental-iterative solution. No matter which solution scheme is selected, the structure needs to be analysed in a consistent reference so that the true loads, displacements, and strains can be calculated. Small-deflection analyses are performed using a Lagrangian reference in which the position of the structure after loading is measured from the original position. For such analyses the deformations are small and the strain-displacement relationship is linear. When combined with a linearly elastic stress-strain relationship, the resultant load-deflection relationship is linear.

The rigid body translations of the nodes become important relative to deformation when displacements are large. In structural analysis there are two generally used methods of dealing with these large displacements, the total Lagrangian formulation and the updated Lagrangian formulation.²⁹ The former uses the Green-Lagrange strain tensor, which contains nonlinear terms, to account for large displacements in the element formulation. The latter permits the use of small-displacement theory by updating the nodal coordinates in a manner that accounts for the large displacements. The updated Lagrangian formulation was selected for this work.

In the updated Lagrangian technique the coordinates in which the elements deform are local coordinates. The orientation of these local coordinates is determined from the current nodal coordinates which are calculated from the displacement results of the most recent increment or iteration. The deformations of the elements due to previous loads are converted to equivalent internal nodal forces and are treated as preload. This preload cancels that part of the applied external load which would cause the existing deformation and leaves only the difference between the external and internal load to cause additional deformation.

Static solution techniques

If the nodal displacements are large, the stiffness matrix becomes a function of the displacements. To solve the nonlinear relations, a residual feedback technique is used.³⁰ The iterative part of the algorithm is derived by expanding

the nonlinear matrix equation in a Taylor series about the displacement vector, q_j , evaluated at an approximate displacement, q_j^{n-1} . A following superscript denotes iteration number and Δq_j^n is a correction to q_j^{n-1} . The displacement vector, q_j^0 is defined as the initial displacement. When only first order terms in the Taylor expansion are retained, and when it is recognized that:

$$\left[\frac{\partial F_i(q_k)}{\partial q_j} \right]^{n-1} = K_{ij}^{n-1} \quad (8)$$

where K_{ij}^{n-1} is the tangent stiffness matrix, the equation becomes:

$$F_i(q_k^{n-1} + \Delta q_k^n) = F_i(q_k)^{n-1} + K_{ij}^{n-1} \Delta q_j^n \quad (9)$$

The load $F_i(q_k)^{n-1}$ is the load required to keep the structure in the shape represented by the displacements q_k^{n-1} and it is equivalent to the internal load R_i^{n-1} caused by these displacements.

The algorithm can be converted to an incremental-iterative scheme by simply defining the first iterations to the stiffness matrix, K_{ij}^0 , and to the internal load vector, R_i^0 , at time, $t + \Delta t$, as those determined at the previous time, t . That is:

$${}^{t+\Delta t}K_{ij}^{n-1} \Delta q_j^n = {}^{t+\Delta t}F_i^n - {}^{t+\Delta t}R_i^{n-1} \quad (10)$$

where a leading superscript denotes increment number; the initial value of the internal load is that determined from the previous convergent load step, and the initial value of the tangent stiffness matrix is also determined from the configuration of the previous step.

Many compliant structures possess an initially low, or zero, stiffness with respect to transverse loads when in their still water configurations. Attempting to solve the stiffness equation without some sort of starting modification results in either a singular matrix or in extremely large estimates of initial displacements and in the probability of slow, or no, convergence.

To accommodate low initial stiffness, the residual feedback scheme has been modified to include viscous relaxation,³⁹ a procedure that gives excellent convergence in cable problems.^{30,39,40} It is implemented by the addition of a viscous drag to the iterative part of the residual feedback algorithm:

$$C_{ij}^n \dot{q}_j + K_{ij}^{n-1} \Delta q_j^n = F_i^n - R_i^n \quad (11)$$

where \dot{q}_j is a vector representing the rate of displacement and C_{ij}^n is an arbitrary damping matrix, usually selected as a constant multiplying the identity matrix, i.e. $C_{ij}^n = C^n \delta_{ij}$, where δ_{ij} is the Kronecker delta. Since the rate of displacement is the change in displacement with respect to two iteration steps, equation (11) may be written as:

$$[C^n \delta_{ij} + K_{ij}^{n-1}] \Delta q_j^n = F_i^n - R_i^n \quad (12)$$

To eliminate the artificial stiffness as the iteration proceeds, the value of C^n is decreased each iteration, i.e.:

$$C^n = \mu C^{n-1} \quad (13)$$

where μ is a decrement parameter specified to give rapid convergence. The selection of μ is problem-dependent and should be chosen by trial and error. The selection of an initial value for C also affects convergence and is adjustable by use of a damping factor, β . In this work C is initially calculated as $C^0 = \beta \text{Min} \langle K_{\text{axial}} \rangle_{\text{elem}}$ where $\langle K_{\text{axial}} \rangle_{\text{elem}}$ is the average of the axial stiffness for all the elements of a particular type. The symbol Min indicates that the least

average stiffness among the element types is used. The selection scheme is purely arbitrary, but it has been shown to give acceptable results.

Dynamic solution techniques

Because of the strong nonlinearity of both the hydrodynamic loading and the structural response, the equation of motion is solved in the time domain. The algorithm selected is the Newmark method, an implicit self-starting scheme which has been used with success for several nonlinear problems.^{30,40,41}

The acceleration is assumed to vary according to some known function during each time step:

$${}^{t+\Delta t}\ddot{q}_i = {}^t\ddot{q}_i + [(1-\zeta){}^t\ddot{q}_i + \zeta{}^{t+\Delta t}\ddot{q}_i] \Delta t \quad (14)$$

and

$${}^{t+\Delta t}q_i = {}^tq_i + {}^t\dot{q}_i \Delta t + [(\frac{1}{2} - \alpha){}^t\ddot{q}_i + \alpha{}^{t+\Delta t}\ddot{q}_i] \Delta t^2 \quad (15)$$

where ζ and α are parameters. Substituting equations (14) and (15) into the equation of motion and solving for ${}^{t+\Delta t}q_j$, one obtains:

$$\hat{K}_{ij} {}^{t+\Delta t}q_j = {}^{t+\Delta t}\hat{F}_{ij} \quad (16)$$

where:

$$\begin{aligned} \hat{K}_{ij} &= a_0 M_{ij} + a_1 C_{ij} + K_{ij} \\ {}^{t+\Delta t}\hat{F}_{ij} &= {}^{t+\Delta t}F_{ij} + M_{ij}(a_0 {}^tq_j + a_2 {}^t\dot{q}_j + a_3 {}^t\ddot{q}_j) \\ &\quad + C_{ij}(a_1 {}^tq_j + a_4 {}^t\dot{q}_j + a_5 {}^t\ddot{q}_j) \end{aligned} \quad (17)$$

and

$$\begin{aligned} a_0 &= \frac{1}{\alpha \Delta t^2} & a_1 &= \frac{\zeta}{\alpha \Delta t} & a_2 &= \frac{1}{\alpha \Delta t} \\ a_3 &= \frac{1}{2\alpha} - 1 & a_4 &= \frac{\zeta}{\alpha} - 1 & a_5 &= \frac{\Delta t}{2} \left(\frac{\zeta}{\alpha} - 2 \right) \end{aligned} \quad (18)$$

Equation (16) constitutes an equivalent static problem from which q_j can be determined. Recommended values of the α and ζ parameters are 0.25 and 0.5, respectively.³⁸ These values provide an unconditionally stable integration scheme for the linear problem and generally provide good stability characteristics for the nonlinear scheme.³⁸ The scheme has not been proved unconditionally stable for all nonlinear problems, but proofs of its unconditional stability for specific problems have been obtained.⁴²

An improved nonlinear integration scheme can be formulated by adopting a residual feedback at each time step. Iteration proceeds until dynamic equilibrium is achieved. If the inertia and damping terms are treated as equivalent loads, the residual feedback scheme may be extended to include damping³⁸ and may be written as:

$$\begin{aligned} {}^{t+\Delta t}M_{ij}^{n-1} {}^{t+\Delta t}q_j^n + {}^{t+\Delta t}C_{ij}^{n-1} {}^{t+\Delta t}q_j^n \\ + {}^{t+\Delta t}K_{ij}^{n-1} \Delta q_j^n = {}^{t+\Delta t}F_{ij}^n - {}^{t+\Delta t}R_{ij}^{n-1} \end{aligned} \quad (19)$$

where:

$${}^{t+\Delta t}q_j^n = {}^{t+\Delta t}q_j^{n-1} + \Delta q_j^n \quad (20)$$

In a manner similar to the derivation of the purely incremental scheme with equation (20) substituted for ${}^{t+\Delta t}q_j$, equation (19) is solved for ${}^{t+\Delta t}\Delta q_j^n$ to obtain:

$$\begin{aligned} {}^{t+\Delta t}\hat{K}_{ij} \Delta q_j^n &= {}^{t+\Delta t}\hat{F}_{ij}^n - {}^{t+\Delta t}R_{ij}^{n-1} \\ &\quad - {}^{t+\Delta t}M_{ij}^n (a_0 {}^{t+\Delta t}q_j^{n-1}) \\ &\quad - {}^{t+\Delta t}C_{ij}^n (a_1 {}^{t+\Delta t}q_j^{n-1}) \end{aligned} \quad (21)_{26}$$

which is the desired recursive formula for an equivalent static problem. The solution to equation (21) then proceeds as was described previously for the combined incremental and iterative statical problem.

The external force F_j^H in equation (4) contains the hydrodynamic drag term:

$$F_j^D = \frac{1}{2} \rho C_D D |V_j^N| (\dot{u}_j^N + \dot{v}_j^N - \dot{q}_j^N) \quad (22)$$

However, \dot{q}_j^N at time $t + \Delta t$ is as yet unknown. If this nonlinear drag term were moved to the left side of equation (19), a nonlinear set of equations would result. This problem is avoided by using a scheme patterned after Anagnostopoulos.⁴³ The value for \dot{q}_j^N is the value calculated from the last time step, ${}^t\dot{q}_j^N$. The force F^D is thus:

$${}^{t+\Delta t}F_i^{Dn} = \frac{1}{2} \rho C_D D |V_i^{Nn}| [{}^{t+\Delta t}(\dot{u}_i^{Nn} + \dot{v}_i^{Nn}) - {}^t\dot{q}_i^N] \quad (23)$$

where:

$$|V_i^N| = \left(\sum_{j=1}^3 ({}^{t+\Delta t}(\dot{u}_j^{Nn} + \dot{v}_j^{Nn}) - {}^t\dot{q}_j^{N(n-1)})^2 \right)^{1/2} \quad (24)$$

The drag component of the hydrodynamic force is thus approximated at the beginning of each iteration but the approximation is upgraded with each subsequent iteration.

Validation problems and results

The computer program developed to implement the algorithms presented in the previous section was validated by a series of test problems.

Problem 1: Steady tow of a cable with sphere

The first problem demonstrates the accuracy of the calculation of hydrodynamic drag forces on the cable element and confirms the validity of neglecting tangential drag forces. The problem was originally presented by Webster⁴⁴ and the experimental curve was determined by Gibbons and Walton.⁴⁵ The structure consists of a long wire terminated by a spherical mass. The wire and mass are towed by a surface vessel at a steady speed of 10.5 knots. The particulars of each of the 10 elements in the model are as follows:

Cable	
Diameter	0.350 in
Submerged weight	0.169 lb/ft
Element lengths	280.0 ft
Total cable length	280.0 ft
$E * A$ value	1.92×10^5 lb
Drag coefficient	1.5
Spherical body	
Diameter	1.0 ft
Submerged weight	580.9 lb
Drag coefficient	0.23

The problem was started with the cable suspended vertically, and viscous relaxation was used. The convergence tolerance was 0.01, the initial artificial damping constant 6860 lb/ft, and the damping and decrement parameters 0.001 and 0.05, respectively. Convergence was reached in 11 iterations. The final configuration at a speed of 10.5 knots is plotted in Figure 1. Webster's results and the experimental results of Gibbons and Walton are also shown.

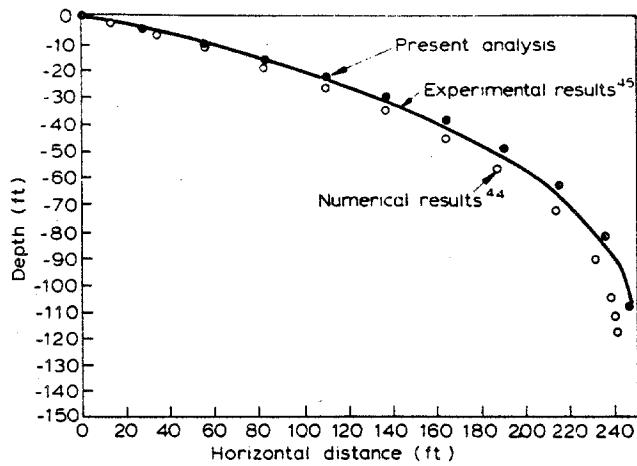


Figure 1 Steady tow of a cable with spherical end mass. Tow speed, 10.0 knots; convergence tolerance, 0.01

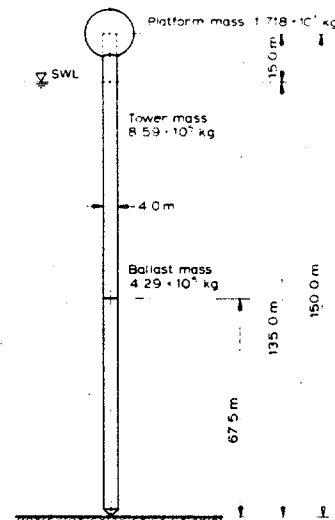


Figure 2 Elevation of articulated tower

The present results compare favourably with the experimental curve. The convergence of the viscous relaxation solution in 11 iterations is a great improvement on the 91 iterations to convergence required by Webster's solution in which viscous relaxation was not used.

Problem 2: Steady current on an articulated tower

A simple articulated tower was modelled and subjected to steady current. The result for steady lean of the tower was then compared to an analytic solution¹ in which the tower was modelled as a rigid body. The model is shown in Figure 2 with geometric and dynamic particulars. The mechanical properties of the shaft are: area = 1.456 m², inertia = 3.580 m⁴, modulus = 2 x 10¹¹ Pa. The drag coefficient used was 0.5 and the inertia coefficient was 2.0.

A steady uniform current of 0.9125 m/s was applied to the tower and the steady angle of inclination was found to be 0.0205 rad. The angle of inclination calculated analytically is also 0.0205 rad. The convergence tolerance used by the program was 0.01. Since the tower has no stiffness in the horizontal directions when in the vertical position, the viscous relaxation option was used to start the solution. The following parameters were used: initial artificial damping constant = 3.9 x 10⁹ N/m, damping factor = 0.000 01, decrement factor = 0.0005. Convergence was reached in five iterations. Figure 3 shows a plot of the solution convergence.

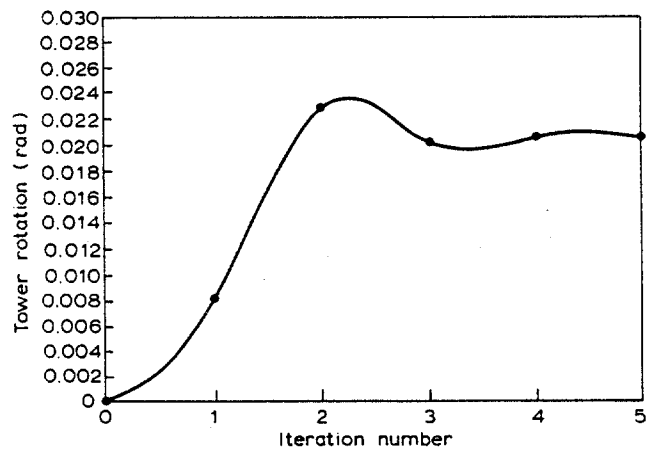


Figure 3 Viscous relaxation solution performance for an articulated tower

Problem 3: Articulated tower in waves

The articulated tower of Problem 2 was subjected to a 30 m, 17 s wave. All parameters were as in Problem 2 except the drag coefficient which was set to 1.0. The time increment was 1.75 s and the convergence tolerance was 0.01.

The response is shown in Figure 4 along with results obtained by Kirk and Jain.¹ There is a difference in the form of the initial response, although the solutions appear to approach each other in the steady-state. Kirk and Jain¹ claimed they required no special starting procedure and that the solution was sufficiently damped to be independent of starting procedure and to give steady-state response almost immediately. They used an explicit integration method as opposed to the implicit Newmark method used in this work. It is not known what the precise reason for the discrepancy is, but it is suspected to be in the difference in the integration methods and starting methods used.

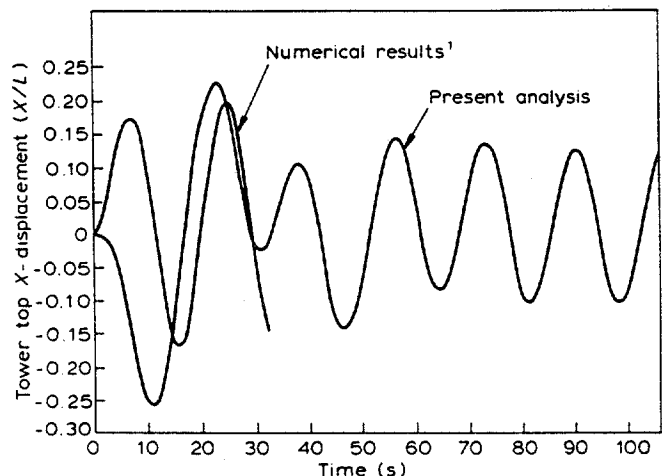


Figure 4 Motion of an articulated tower in waves only. Wave, 30 m-17 s; convergence tolerance, 0.01; time step, 1.75 s; CPU time/real time, 1.35

To obtain an idea of the dynamic response of the tower, it was leaned to the maximum amplitude of excursion from the previous problem, and released. The convergence tolerance was again 0.01. The dynamic response is shown in Figure 5. The logarithmic decrement was measured for each half cycle and the effective damping parameter calculated. The results are tabulated below.

Half cycle	Damping factor, ξ
1	—
2	0.17
3	0.09
4	0.08
5	0.06

These results indicate a system that is not heavily damped, as would be implied by the results of Kirk and Jain.¹ The present results were determined, however, using the Newmark integration scheme, so the results are not independent. When the forced results are compared with the free oscillation results, the undulation of the forced results fits well with the undulation of the free oscillation results, as would be expected, leading one to believe that the algorithm is functioning properly.

The articulated tower was subjected to a 30 m, 17 s wave plus a 0.9125 m/s current moving at 90 degrees to the wave direction. Calculated x - y motion of the tower top and the Kirk and Jain results¹ are shown in Figure 6. Again, the initial amplitudes are large, but the motion of the tower predicted by the present algorithm is otherwise very similar to the results of Kirk and Jain.¹

Problem 4: Two-dimensional guyed tower in waves

A two-dimensional model of a guyed tower was formulated to demonstrate the use of beam, cable, and foundation elements and to demonstrate solutions in which some of the elements are assumed to participate in a quasi-static manner. A definition sketch is shown in Figure 7. The tower was modelled as two beam elements, one extending from the pinned base to the guy connection and one from the point of guy connection to the deck mass. The two guys were each modelled as three cable elements terminated at the sea floor by a foundation spring whose hori-

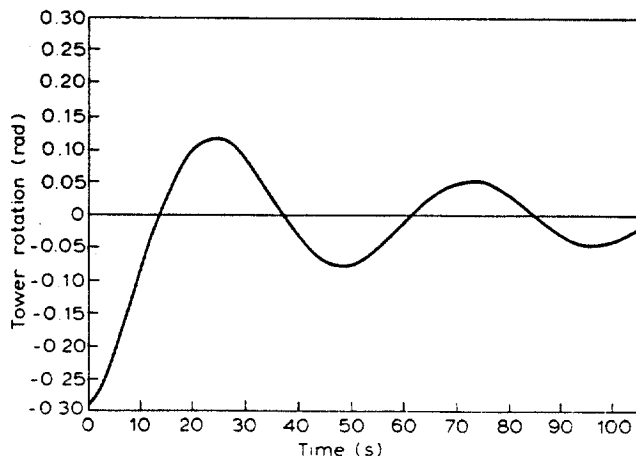


Figure 5 Free oscillation of an articulated tower in still water. Convergence tolerance, 0.01; time step, 1.75 s; CPU time/real time, 1.12

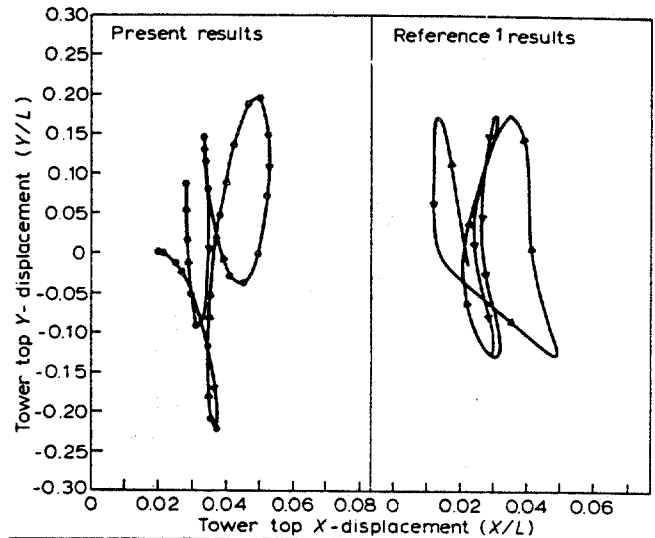


Figure 6 Motion of an articulated tower in waves and transverse current. Wave, 30 m-17 s; current, 0.9125 m/s; time step, 0.5 s; convergence tolerance, 0.01; CPU time/real time, 4.03

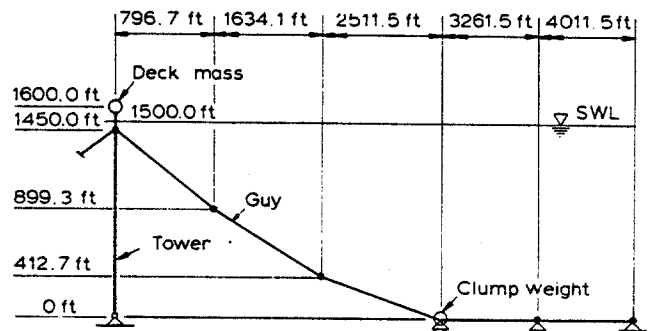


Figure 7 Elevation of guyed tower model

zontal stiffness was equivalent to that of the length of cable which usually extends from the clump weight to the guy anchor. The physical properties of the model used in the analysis were as follows:

Environment		Deck	
Water depth	1500 ft	Mass	466.4 k slugs
Wave period	10 s	Rotational inertia	0
Wave height	30 ft		
Column			
Mass density			0.00249 k slug/ft ³
Weight density			0.0160 kip/ft ³
Elastic modulus			4.176 × 10 ⁶ kip/ft ²
Cross-sectional area			62.8 ft ²
Second moment of the area (about x_2 - x_2' and x_3 - x_3' axes)			1.571 × 10 ⁵ ft ⁴
Torsional constant			3.142 × 10 ⁴ ft ⁴
Displaced volume			312.5 ft ³ /ft
Drag width			115.0 ft
Drag coefficient			0.7
Inertia coefficient			1.814
Guys			
Mass density			0.01524 k slug/ft ³
Weight density			0.426 kip/ft ³

Coupled response of compliant offshore platforms: J. W. Leonard and R. A. Young

Elastic modulus	0.43×10^7 kip/ft ²
Cross-sectional area	0.3341 ft ²
Displaced volume	0.3341 ft ³ /ft
Drag width	1.458 ft
Drag coefficient	0.7
Inertia coefficient	2.0
Initial tension at tower	1250 kip

Foundation springs

Horizontal stiffness	957.7 kip/ft
Vertical stiffness	1×10^{14} kip/ft

For the solution in which quasi-static cables were assumed, the mass density, drag coefficient and inertia coefficient of the cables were set equal to zero so that the cables performed as static catenary springs. The time step selected was 0.5 s and a convergence tolerance of 0.01 was used.

The horizontal displacements of the deck for both the dynamic and the quasi-static solutions are shown in Figure 8. The quasi-static solution is seen to overpredict the amplitude of deck movement by 20-100% in the 45 s of data plotted. These results imply that the deck accelerations are overpredicted when the guys are modelled as springs.

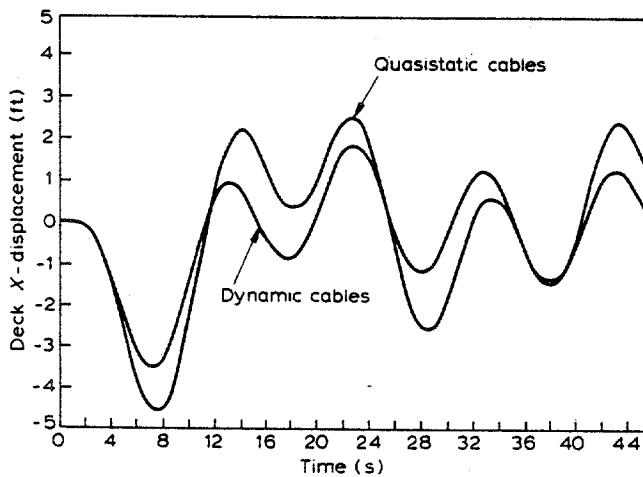


Figure 8 Transverse displacement of guyed tower deck vs. time. Wave 30 ft-10 s; convergence tolerance, 0.01; time step, 0.5 s; CPU time/real time, 6.71

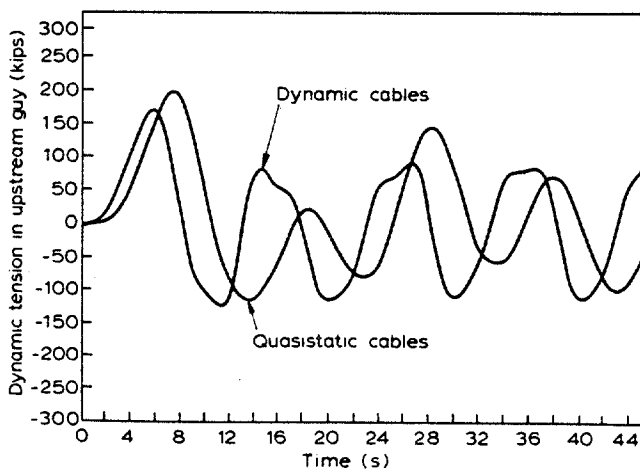


Figure 9 Guy tension vs. time

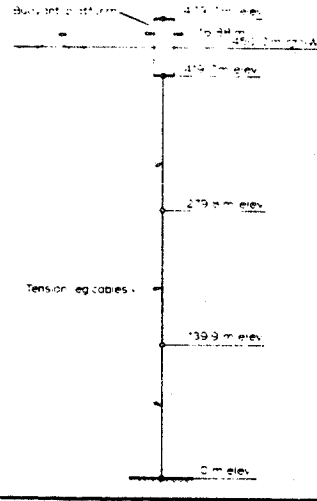


Figure 10 Tension leg structure

The guy tensions at the connection point for the dynamic and the quasi-static solutions are plotted in Figure 9. The quasi-static solution overpredicts the peak tension and the times at which peak loadings occur are significantly different. The shape of the dynamic trace of the load is attributable to the spatial dependence of hydrodynamic loading on the guys.

Problem 5: Tension-leg structure in waves

A simplified tension-leg structure was subjected to waves as an additional demonstration of the versatility of the techniques employed in this work. A surface piercing cylindrical buoy was moored to the bottom by a single cable (see Figure 10). The particulars are as follows:

Column

Mass density	0.2529 kg/m ³
Weight density	1.229 N/m ³
Elastic modulus	2.1×10^8 N/m ²
Cross-sectional area	2.066 m ²
Second moment of area	75.55 m ⁴
Torsional constant	151.3 m ⁴
Displaced volume	223.8 m ³ /m
Drag width	16.88 m
Drag coefficient	0.7
Inertia coefficient	2.0

Cables

Mass density	1.023 kg/m ³
Weight density	10.03 N/m ³
Elastic modulus	2.1×10^8 N/m ²
Cross-sectional area	0.397 m ²
Displaced volume	0.397 m ³ /m
Drag width	1.422 m
Drag coefficient	0.7
Inertia coefficient	2.0

Viscous relaxation was used to obtain the inertial equilibrium position of the structure. The parameters are as follows: initial artificial damping constant = 596 139 nt/m/s, damping factor = 1.0, decrement factor = 0.05, water depth = 450 m, wave period = 15 s, wave height = 15 m. The time step selected was 0.5 s and the convergence tolerance was 0.01.

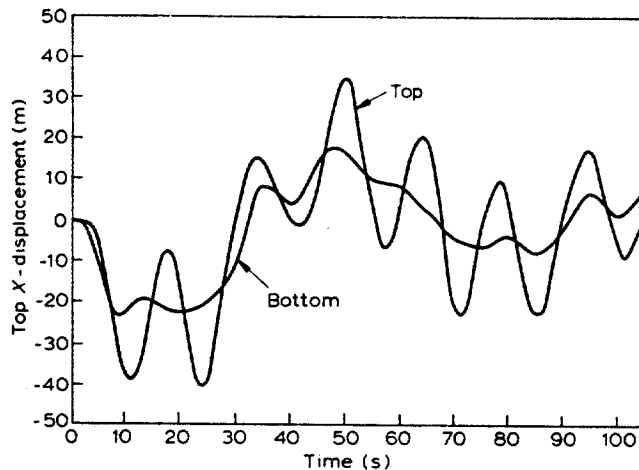


Figure 11 Transverse displacement of tension leg structure vs. time. Wave 15 m-15 s; convergence tolerance, 0.01; CPU time/real time, 3.96

The horizontal displacement of the cylinder top and bottom are plotted in Figure 11. The bottom of the cylinder, being restrained by the tether, shows a more attenuated response at the wave frequency than does the top of the cylinder. The response appears stable and appears to be approaching steady state at the conclusion of the time record.

Conclusions

A three-dimensional, large-deflection finite element program has been developed which is capable of simulating the static and dynamic behaviour of large compliant ocean structures. The structures are assumed to be in the Morison regime and to be composed of cable and beam-column elements. No vortex shedding, diffraction effects, nor material nonlinearities are considered. Linear wave theory is used and multidirectional irregular seas may be simulated by a series of regular waves. Current may be included as an arbitrary current profile varying in magnitude and direction with depth. Concentrated masses and loads as well as foundation properties may also be modelled.

The use of updated Lagrangian coordinates and a residual feedback solution scheme has been shown to be a valid technique for solving the geometrically nonlinear problem. Static problems indicate that the scheme yields excellent results in comparison to available theoretical solutions. Furthermore, these results were obtained with liberal convergence tolerances and large element discretizations.

It has been confirmed that the viscous relaxation method is an excellent method to start the static solution of hardening nonlinear problems with little or no initial stiffness in one or more degrees-of-freedom. The method is particularly efficient when used on articulated structures which use buoyancy for stability. More iterations are required when the method is used on cable problems and on problems using both cables and beams, but the technique is still superior to dynamic relaxation⁷ for the examples considered in this work.

The selection of the coefficients in the relaxation process depends upon experience. However, some observations can be made to determine if the selected coefficients are adequate and if they can be improved. If insufficient initial stiffness is added, the structure remains unstable and

this instability will be exhibited in the first iteration by a zero or negative pivot during reduction of the equations. If the decrement factor is too small, a similar situation will occur in a subsequent iteration. Conversely, if the decrement factor is large and the initial stiffness is large, the convergence plot will appear like the free response of an overdamped system subject to a step load and the solution will converge exponentially. An optimum solution appears like the free response of an underdamped system and exhibits some overshoot, as in Figure 3, but a heavily damped solution resulting from large initial artificial stiffness and a large decrement factor will permit a solution to be obtained only at the expense of additional iteration cycles.

The iterative Newmark method has been shown to provide good solutions to nonlinear dynamic problems in the time domain even at time steps and convergence tolerances which are large compared to those often suggested in the literature. The algorithm has been shown to give reasonable results for hydrodynamic solutions. However, although these results are similar to published results, there is enough disparity to warrant investigation of the performance of this and other algorithms compared to experimental results.

Results of the guyed tower show that for the examples presented, the use of static spring models of the guys leads to an overprediction of the tower motion and also of the guy tensions. There is also a large difference in the time phase of the tensions and in the form of the tension versus time plots. The tension-leg problem demonstrates that the algorithms are capable of handling tension-leg structures and that the solution is stable over a long time history.

In general the algorithms selected and used in this work perform in a manner which is satisfactory for their intended function. The techniques require a considerable amount of computer time to obtain solutions compared to the computer time usually required by linear analyses. As the nonlinearities increase in strength, the computer time for similar problems increases greatly but there is no apparent degradation in the accuracy of the results for the test problems considered.

Acknowledgements

This investigation was funded in part by the Minerals Management Service and the National Bureau of Standards of the US Department of the Interior through Grant No. NB82NADA3008. Computer funds were provided by the Oregon State University Computer Center.

References

- 1 Kirk, C. L. and Jain, R. K. 'Response of articulated towers to waves and current', *Proc. Offshore Technol. Conf.*, Houston, TX, 1977, Paper no. 2798
- 2 Jain, R. K. and Kirk, C. L. 'Dynamic response of a double articulated offshore loading structure to noncollinear wave and current', *ASME J. Energy Resour. Tech.*, 1981, 103 (1)
- 3 Chakrabarti, S. K. and Cotter, D. C. 'Transverse motion of articulated tower', *ASCE J. Waterways Port, Coastal and Ocean Div.*, 1980, 106 (1)
- 4 Finn, L. D. and Young, K. E. 'Field test of a guyed tower', *Proc. Offshore Technol. Conf.*, Houston, TX, 1978, Paper no. 3131
- 5 Finn, L. D. 'A new deepwater offshore platform - the guyed tower', *Proc. Offshore Technol. Conf.*, 1976, Paper no. 2688

Coupled response of compliant offshore platforms: J. W. Leonard and R. A. Young

- 6 Mes, M. J. 'Guyed tower design and analysis, Parts 1-5', *Petroleum Eng. Int.*, 1981-1982, 53 (13)
- 7 Smith, E., Aas-Jakobsen, A. and Sigborsson, R. 'Nonlinear stochastic analysis of compliant platforms', *Proc. Offshore Technol. Conf.*, 1980, Paper no. 3801
- 8 Triantafyllou, G. Karkomateas and Blick, A. 'The statics and dynamics of the mooring lines of a guyed tower for design applications', *Proc. BOSS '82*, 1982, 1, 546
- 9 MacDonald, R. D. 'The design and field testing of the 'Triton' tension leg fixed platform and its future application of petroleum production and processing in deep water', *Proc. Offshore Technol. Conf.*, Houston, TX, 1974, Paper no. 2104
- 10 Pauling, J. R. and Horton, E. E. 'Analysis of tension leg stable platform', *Proc. Offshore Technol. Conf.*, 1970, Paper no. 1263
- 11 Rainey, R. C. T. 'The dynamics of tethered platforms', *Trans. Royal Inst. Naval Architects*, 120, London, England, 1978
- 12 Rainey, R. C. T. 'Parasitic motions of offshore structures', *Trans. Royal Inst. Naval Architects*, 122, London, England, 1980
- 13 Albrecht, H. G., Koenig, D. and Kokkinowrachos, K. 'Non-linear analysis of tension leg platforms for medium and greater depths', *Proc. Offshore Technol. Conf.*, Houston, TX, 1978, Paper no. 3044
- 14 De Zoysa, 'Steady state analysis of undersea cables', *Ocean Eng.*, 1978, 5 (3), 00
- 15 McIver, D. B. 'The static offset of tension leg platforms', *Proc. Offshore Technol. Conf.*, 1981, Paper no. 4070
- 16 Yoshida, K., Koneya, T., Oka, N. and Ozaki, M. 'Motions and leg tensions of tension leg platforms', *Proc. Offshore Technol. Conf.*, Houston, TX, 1981, Paper no. 4073
- 17 Jefferys, E. R. and Patel, M. H. 'Dynamic analysis models of the tension leg platform', *Proc. Offshore Technol. Conf.*, Houston, TX, 1981, Paper no. 4075
- 18 Natvig, B. J. and Pendered, J. W. 'Nonlinear motion response of floating structures to wave excitation', *Proc. Offshore Technol. Conf.*, Houston, TX, 1977, Paper no. 2796
- 19 Ashford, R. A. and Wood, W. L. 'Numerical integration of the motions of a tethered buoyant platform', *Int. J. for Numer. Methods in Eng.*, 1978, 13, 165
- 20 Gie, T. S. and de Boom, W. C. 'The wave induced motions of a tension leg platform in deep water', *Proc. Offshore Technol. Conf.*, Houston, TX, 1981, Paper no. 4074
- 21 Penzien, J. 'Structural dynamics of fixed offshore structures', *Behavior of Offshore Structures, Proc. 1st Int. Conf.*, 1976, 1, 581
- 22 Taudin, P. 'Dynamic response of flexible offshore structures to regular waves', *Proc. Offshore Technol. Conf.*, 1978, Paper no. 3160
- 23 Fish, P. R., Dean, R. B. and Heaf, N. J. 'Fluid-structure interaction in Morison's equation for the design of offshore structures', *Eng. Struct.*, 1980, 2 (1), 15
- 24 Fish, P. R. and Rainey, R. 'The importance of structural motion in the calculation of wave loads', *Behaviour of offshore structures, Proc. 2nd Int. Conf.*, London, UK, 1979, 2, 43
- 25 Ansari, K. A. 'Mooring with multicomponent cable systems', *ASME J. Energy Resource Tech.*, 1980, 102 (2)
- 26 Suhara, T. et al. 'Dynamic behavior and tension of oscillating mooring chain', *Proc. Offshore Technol. Conf.*, 1981, Paper no. 4053
- 27 Peyrot, A. H. 'Marine cable structures', *ASCE J. Struct. Div.*, 1980, 106 (12)
- 28 Wilhelmly, V., Fjeld, S. and Schneider, S. 'Non-linear response analysis of anchorage systems for compliant deep water platforms', *Proc. Offshore Technol. Conf.*, 1981, Paper no. 4051
- 29 Cook, R. D. 'Concepts and applications of finite element analysis', 2nd Edn, John Wiley and Sons, 1981
- 30 Tuah, H. 'Cable dynamics in an ocean environment', *PhD Thesis*, Oregon State University, Corvallis, OR, 1982
- 31 Wade, B. G. and Dwyer, M. 'On the application of Morison's equation to fixed offshore platforms', *Proc. Offshore Technol. Conf.*, 1976, Paper no. 2723
- 32 Morison, J. R., O'Brien, M. P., Johnson, J. W. and Schaff, S. A. 'The force exerted by surface waves on piles', *Petroleum Trans., AIME*, 1950, 189, 149
- 33 Sarpkaya, T. and Isaacson, M. 'Mechanics of wave forces on structures', Van Nostrand Reinhold, NY, 1981
- 34 Berteaux, H. O. 'Buoy engineering', John Wiley and Sons, 1976
- 35 Dalrymple, R. A. 'Models for nonlinear water waves on shear currents', *Proc. Offshore Technol. Conf.*, 1974, Paper no. 2114
- 36 Leonard, J. W. and Hudspeth, R. T. 'Loads on sea-based structures', *Structural Technol. in the Ocean, ASCE Natl. Convention*, Atlanta, GA, 1979
- 37 Biesel, F. 'Etude theoretique de la houle en eau courante', *La Houille Blanche*, 1950, 5A, 279
- 38 Bathe, K. 'Finite element procedures in engineering analysis', Prentice-Hall, 1982
- 39 Webster, R. L. 'On the static analysis of structures with strong geometric nonlinearity', *Computers and Structures*, 1980, 11, 137
- 40 Lo, A. 'Nonlinear dynamic analysis of cable and membrane structures', *PhD Thesis*, Oregon State University, Corvallis, OR, 1982
- 41 Bathe, K., Ramm, E. and Wilson, E. L. 'Finite element formulations for large deformation dynamic analysis', *Int. J. for Numer. Methods in Eng.*, 1975, 9, 353
- 42 Belytschko, T. and Schoeberle, D. F. 'On the unconditional stability of an implicit algorithm for nonlinear structural dynamics', *J. Applied Mech.*, 1975, 97, 865
- 43 Anagnostopoulos, S. W. 'Dynamic response of offshore platforms to extreme waves including fluid-structure interaction', *Eng. Struct.*, 1982, 4, 179
- 44 Webster, R. L. 'Nonlinear static and dynamic response of underwater cable structures using the finite element method', *Proc. Offshore Technol. Conf.*, 1975, Paper no. 2322
- 45 Gibbons, T. and Walton, C. O. 'Evaluation of two methods for predicting tensions and configurations of a towed body system using bare cable', *David Taylor Model Basin Report 2313*, 1966